Journal of Cranio-Maxillo-Facial Surgery 47 (2019) 185–189

Contents lists available at ScienceDirect

Journal of Cranio-Maxillo-Facial Surgery

journal homepage: www.jcmfs.com

A simple method to estimate the linear length of the orbital floor in complex orbital surgery☆

Konstantinos Natsis [a], Maria Piagkou [b, *], Ioannis Chryssanthou [b], Georgios P. Skandalakis [b], Georgios Tsakotos [b], Giannoulis Piagkos [b], Constantinus Politis [c, d]

[a] Department of Anatomy and Surgical Anatomy, (Chairperson: Professor Dr. K. NATSIS), Medical School, Aristotle University of Thessaloniki, Greece
[b] Department of Anatomy, (Chairperson: Professor Dr. P. SKANDALAKIS), Medical School, National and Kapodistrian University of Athens, Greece
[c] OMFS-IMPATH Research Group Department of Imaging and Pathology, (Chairperson: Professor Dr. C. Politis), Belgium
[d] Department of Oral and Maxillofacial Surgery, Hasselt University, Diepenbeek, Belgium

ARTICLE INFO

Article history:
Paper received 3 June 2018
Accepted 2 November 2018
Available online 9 November 2018

Keywords:
Orbital floor
Infraorbital rim
Orbit
Formula
Orbital surgery
Reconstruction

ABSTRACT

Background: The orbital floor (OrF) and infraorbital rim (IOR) repair in cases of complete destruction is challenging mainly due to the fact that the defect length cannot be measured. The aim of the current study is to develop a method of calculating the Orf length by using the gender and the lengths of the medial, superior and lateral orbital walls (OrW) of the same orbit.
Material and methods: Ninety-seven (59 male and 38 female) European adult dry skulls were classified according to age: 20–39, 40–59 and 60 years and above. The length of each OrW was measured by using the direct distance between the optic foramen and a landmark in each orbital rim.
Results: A side asymmetry was detected for the lengths of the inferior, superior and medial OrW. Although a gender dimorphism was detected, no correlation with the age was found. Using the Stepwise multiple regression analysis two formulas were developed, one for the right and one for the left OrF with coefficient of determination R^2 0.43 and 0.57, respectively.
Conclusions: The proposed formulas represent a simple, applicable and individualized method to calculate the OrF linear length in cases of complete destruction of the IOR and OrF, with accuracy and without the use of expertise material. Such data may improve the surgery planning of orbital floor fractures and complex orbital reconstructions.

1. Introduction

The bony orbit is one of the most complex areas of the skull (Hatcher, 2012) and is composed of four orbital walls (OrW) (roof, floor, lateral and medial walls). The orbital floor (OrF) is bounded by the maxillo-ethmoidal strut medially, by the infraorbital fissure laterally, by the optic foramen (OF) posteriorly and by the infraorbital rim (IOR) anteriorly (Turvey and Golden, 2012). The main part of the OrF is formed by the orbital plate of the maxilla, while a part of the palatine and the zygomatic bones contribute posteriorly and anterolaterally to the OrF (Balasubramanian, 2011). The anterior surface of the OrF which is constituted by cortical bone is thick, while the area of the maxillary sinus expansion is particularly thin (Roth et al., 2010; Turvey and Golden, 2012).

The OrF and IOR may be simultaneously destructed by a plethora of pathological entities, such as trauma [combined intra-orbital and orbital rim fractures (Markiewicz and Bell, 2012; Reyes et al., 2013), gunshots (Liliav and Kalimuthu, 2012)] and tumors (benign-eosinophilic granuloma, leiomyoma, primary intraosseous hemangioma, osteoblastoma and Giant-cell tumor and malignant-rhabdomyosarcoma, neuroblastoma, osteosarcoma, chondrosarcoma, Ewing sarcoma, fibrosarcoma and metastatic tumors) (Razek, 2011; Yan et al., 2012). Injury of the OrF and IOR may lead to various functional and aesthetic complications that profoundly affect the quality of life and well-being of the patient. Thus, the

☆ The work should be attributed to the Department of Anatomy and Surgical Anatomy of the Medical School of the Aristotle University of Thessaloniki (*Head of the Department, Konstantinos Natsis*).

* Corresponding author. Department of Anatomy, School of Medicine, National and Kapodistrian University of Athens, M. Asias 75 Street, 11527, Goudi, Athens, Greece.
E-mail address: mapian@med.uoa.gr (M. Piagkou).

https://doi.org/10.1016/j.jcms.2018.11.001
1010-5182/

repair of the affected OrF in its exact previous morphology is crucial (Peng et al., 2017; Markiewicz and Bell, 2012). In order to achieve this goal, the knowledge of the OrF length and bony contour prior to the injury is required. However, in cases of extensive destruction, the reconstruction is extremely challenging (Nillson et al., 2018; Markiewicz and Bell, 2012). In an effort to achieve the previous shape of the affected orbit, a three-dimensional (3D) computed tomography (CT) scan has been used to depict the uninjured side, using it as a mirror-image for the reconstruction of the contralateral injured side (Novelli et al., 2014; Fang et al., 2013; Bell and Markiewicz, 2009). Even though the mirroring technique is promising, the computer models are not widely available (Szymor et al., 2016), they are costly and their use requires computer expertise (Metzger et al., 2006). Mirroring further assumes equal bony relations and distances between affected and unaffected side.

The aim of the current study conducted in European dry skulls was to investigate the side differences of the OrF lengths; to estimate the OrF length in a single orbit by using the lengths of the medial, superior and lateral OrW of the same orbit; and to develop an easy method of calculation of the OrF length. The estimated length could then be used to check the result of the mirrored OrF length in order to prevent the choice of a too long prefabricated orbital floor implant.

2. Material and methods

Ninety-seven skulls (194 orbits) of a European modern adult population were examined. The sample consisted of disarticulated skeletons that were randomly selected from a cemetery for research purposes and belonged to individuals who died between 1951 and 2000. Children, unknown and orbits with apparent abnormalities were not included in the current study, as they may cause morphological changes that affect the relationship between normal osseous structures of the orbit. The age at the time of death and the gender of all specimens were known. The current research was approved by the Research Ethics Committee of our Institutions. The 59 male and 38 female skulls were classified into three groups according to age: 20–39 (21 skulls), 40–59 (36 skulls) and 60 years and above (40 skulls).

Considering that the OrF is a part of the orbital cavity, we hypothesized that its length may have a direct correlation to the lengths of the other OrWs of the same orbit. The lengths of the OrW can be calculated only after the assumption of the conical shape of the orbit. The OF represents the apex of the cone and the base is formed from the supraorbital rim, the anterior lacrimal crest, the infraorbital and the lateral orbital rims. The OrWs extend from each orbital rim to the OF. Thus, for the OrW length measurement, a constant osseous landmark was selected in each orbital rim and from this point the linear distance to the OF was measured. The lengths measurements were as follows (Fig. 1):

1. On the orbital roof, the distance from the inferior border of the supraorbital foramen or notch (SOF/N) to the midpoint of the superior border of the OF, (SOF/N -OF)
2. On the orbital floor, the distance from the crossing point of the zygomaticomaxillary suture (ZMS) and the IOR to the midpoint of the inferior border of the OF, (ZMS-OF)
3. On the lateral OrW, the distance from the inner border of the frontozygomatic suture (FZS) to the midpoint of the lateral border of the OF, (FZS-OF)
4. On the medial OrW, the distance from the midpoint of the anterior lacrimal crest (MALC) (using the largest opening of the nasolacrimal duct as a reference point) to the midpoint of the medial border of the OF, (MALC-OF).

All measurements were made by using a flexible wire that was adopted between the above landmarks and then its length was calculated with a digital caliper (accuracy 0.01 mm). All the above measurements were performed in the intact OrWs of each orbit.

2.1. Statistical analysis

The Wilcoxon test was performed for side symmetry. Mann–Whitney test and the Independent sample t-test were used to investigate gender dimorphism. ANOVA and Kruskall–Wallis test were used for the correlation of the above parameters with the age. The Pearson correlation was used to assess correlations between the OrF length and the other orbital lengths. The multiple regression analysis with a stepwise approach was used to investigate the possibility of prediction of the OrF length using the other measurements as independent variables. The statistical analysis was performed using the SPSS for Windows version 20.0. The level of statistical significance was considered at $p \leq 0.05$.

3. Results

Descriptive statistics of the OrW lengths (mean ± SD, median, minimum and maximum) are summarized in Table 1.

3.1. Statistical analysis regarding the side symmetry, gender and age

The values for the ZMS-OF were 46.42 mm on the right and 45.30 ± 2.65 mm on the left side with a statistically significant right dominance ($p = 0.0001$). The lengths MALC-OF ($p = 0.0001$) were longer on the right side, while the SOF/N-OF presented a left side preponderance ($p = 0.0001$). A side symmetry was observed, concerning the FZS-OF ($p = 0.106$). A gender dimorphism was observed in all the measured parameters with a male preponderance. The ZMS-OF lengths of male and female orbits were 47.32 ± 3.37 mm and 45.36 ± 2.39 mm on the right side ($p = 0.002$) and 46.29 ± 2.64 mm and 43.92 ± 2.01 mm on the left side ($p = 0.0001$), respectively. No correlation was found between the OrW lengths and the age.

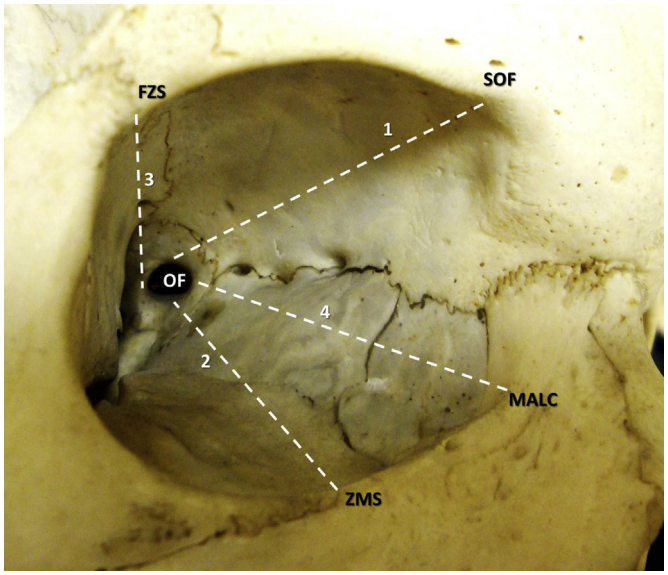

Fig. 1. The measurement of the length of each orbital wall.

Table 1
Descriptive statistics of the orbital walls lengths according to side.

Lengths	N	p*	Right			N	p*	Left			p**
			Mean ± SD	Median	Min- Max			Mean ± SD	Median	Min-Max	
SOF/N-OF	92	0.200	42.19 ± 2.71	42.14	35.45–47.51	90	0.0001	43.46 ± 4.34	43.26	36.65–75.00	0.0001
ZMS-OF	92	0.005	46.93 ± 3.15	46.42	37.82–62.00	90	0.116	45.28 ± 2.68	45.70	40.62–51.99	0.0001
FZS-OF	92	0.200	42.90 ± 2.52	42.84	36.45–48.97	90	0.0001	43.23 ± 4.87	42.42	37.92–74.00	0.106
MALC-OF	91	0.0001	41.55 ± 3.10	41.39	25.05–47.66	88	0.200	41.03 ± 2.47	41.17	33.87–46.57	0.0001

N: number of the orbits measured, *: p value of the Kolmogorov–Smirnov test investigates the normality of the distribution, **: p value of the Wilcoxon test.

3.2. Pearson correlation analysis

The Pearson correlation analysis between the OrF length and the other OrW lengths was performed on the right and left sides. A strong positive linear correlation was observed between the OrF length and the lengths of the other OrWs (FZS-OF, SOF/N-OF and MALC-OF), on both sides with a level of significance at $p \leq 0.01$. Thus, our hypothesis is confirmed (Table 2).

3.3. Multiple regression analysis

The multiple regression analysis was performed to investigate the possibility of predicting the OrF length. In particular, a formula that could predict the OrF length (dependent variable) by using as independent variables the other orbital parameters of the same orbit was developed. The goal was to create a formula that would combine a high coefficient of determination (R^2) and fewer possible independent variables for an easier application. Thus, the stepwise approach was selected in order to find the best combination of independent variables that could predict the dependent variable. The gender (0 = males, 1 = females), the age (divided in two dummy variables) and the OrWs measurements (FZS-OF, SOF/N-OF and MALC-OF) were used as independent variables in our model. The correlations between variables were analysed for the existence of multicollinearity (tolerance and vide infra-VIF) and no variable was excluded. The multiple regression analysis was performed separately for the right and left orbit as side asymmetry was detected, and as a result two formulas were created.

Using the regression analysis for the length of the right-sided OrF, the MALC-OF was the first independent variable entered in the model and thus it was the largest predictor of the right-sided OrF length. The SOF/N-OF was the second (and last) variable entered in the model and together these variables statistically significantly predict the OrF length, $F(6, 97) = 28.82$, $p < 0.0001$, $R^2 = 0.43$ (Table 3). The equitation developed for the prediction of the right-sided OrF length was: ZMS-OF right (mm) = 11.557 + 0.532 × MALC-OF right (mm) + 0.305× SOF/N-OF right (mm). A similar procedure was followed for the left-sided OrF length. The independent variables entered in the model in order of statistical significance were: MALC-OF, SOF/N-OF, gender and FZS-OF. These variables statistically significantly predict the left-sided OrF length, $F(6, 97) = 24.86$, $p < 0.0001$, $R^2 = 0.57$ (Table 3).

The equitation developed for the prediction of the left-sided OrF length was: ZMS-OF left (mm) = 12.308 + 0.342 × MALC-OF left (mm) + 0.264 × SOF/N–OF left- 1.01x gender + 0.189 × FZS-OF left (mm). The relationships between the measured OrF lengths and the predicted OrF lengths by the above formulas on the right and left sides are shown in Fig. 2a and b.

4. Discussion

The OrF is an area commonly affected after a traumatic or neoplastic event. When the affected area is posterior to an intact IOR, the implant size can be easily measured either by calculating the dimensions of the defect using the CT scan of the affected orbit (Piombino et al., 2010) or by using a waterproof paper ruler, intraoperatively (Lim et al., 2012). In cases of complete destruction of the OrF including the IOR, the above measurement techniques cannot be used and methods such as the mirroring technique and the use of the 3-dimensional pre-bent titanium mesh implants are more appropriate (Metzger et al., 2006; Bell and Markiewicz, 2009). The above two techniques estimate with accuracy the implant dimensions and the native bony contour, but some disadvantages limit their use. The 3-D pre-bent titanium mesh technique requires aluminum molds that are not individualized as only twelve different patterns are used. The mirroring technique apart from the fact that it is quite costly and requires computer expertise is based on the assumption of the orbital symmetry. Our results warrant caution if the OrF length is used based on the mirroring technique without checking the reference landmarks on the affected side as proposed.

In an effort to find a technique more easily applicable, we developed a formula for the calculation of the OrF length that does not require the use of expertise materials. Firstly we investigated

Table 2
Pearson correlations between the orbital floor (OrF) length and the other orbital walls (OrWs) lengths on the right and left side.

	r	p
Right		
ZMS-OF and FZS-OF	0.539	0.0001
ZMS-OF and MALC-OF	0.563	0.0001
ZMS-OF and SOF/N-OF	0.554	0.0001
Left		
ZMS-OF and FZS-OF	0.542	0.0001
ZMS-OF and MALC-OF	0.652	0.0001
ZMS-OF and SOF/N-OF	0.618	0.0001

ZMS- zygomaticomaxillary suture, OF-orbital floor, FZS-frontozygomatic suture, MALC- midpoint of the anterior lacrimal crest, SOF/N- supraorbital foramen or notch.

Table 3
The parameters of the multiple regression analysis of the orbital floor length using as independent variables the MALC-OF and SOF/N-OF on the right and MALC-OF, SOF/N-OF, gender and FZS-OF on the left side.

Variables	B	SE*	p	CI**
Right				
(Constant)	11.557	4.622	0.015	2.355–20.759
MALC-OF	0.532	0.120	0.0001	0.293–0.771
SOF/N-OF	0.305	0.101	0.003	0.105–0.506
Left				
(Constant)	12.308	4.368	0.006	3.606–21.010
MALC-OF	0.342	0.116	0.004	0.110–0.573
SOF/N-OF	0.264	0.113	0.022	0.039–0.389
Gender	−1.01	0.454	0.029	−1.913–(−0.105)
FZS-OF	0.189	0.194	0.049	0.001–0.377

* SE = standard error, ** CI = 95% coefficient interval for B.
ZMS- zygomaticomaxillary suture, OF-orbital floor, FZS-frontozygomatic suture, MALC- midpoint of the anterior lacrimal crest, SOF/N- supraorbital foramen or notch.

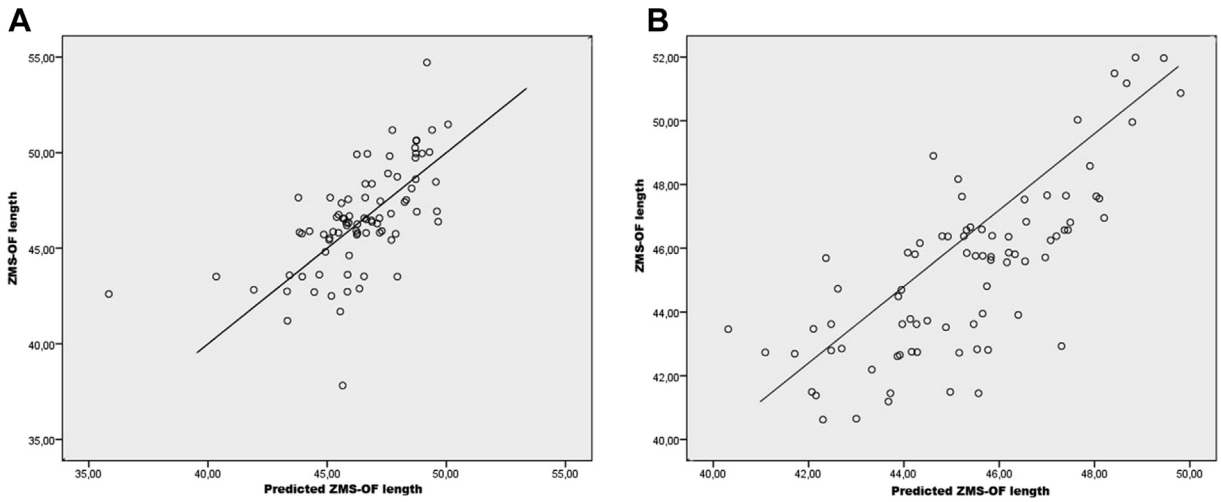

Fig. 2. A- The relationship between the measured orbital floor (OrF) lengths and the predicted OrF lengths by the above formulas on the right side. **B**- The relationship between the measured orbital floor (OrF) lengths and the predicted OrF lengths by the above formulas on the left side.

the occurrence of side symmetry between the orbital lengths. An important finding of the current study was the existence of side asymmetry regarding the OrWs lengths (ZMS-OF, MALC-OF and SOF/N-OF). This finding indicates that the use of the OrF length of an orbit for the depiction of the contralateral OrF length is inaccurate. As a result, we developed two different formulas, one for each side of the OrF length that included only variables of the same side. In particular, the parameters used for the measurement of the right-sided OrF length were the MALC-OF and the SOF/N-OF and for the left-sided OrF length were the MALC-OF, the SOF/N-OF, the gender and the FZS-OF. The main advantage of our technique is the calculation of the OrF length measuring only three parameters in a CT scan without the use of any additional material.

The use of the appropriate implant size is of paramount importance for a favourable aesthetic and functional outcome of the orbital repair. In order to avoid the major complication of the implant migration and achieve the pre-damaged orbital status, an implant of the exact length with the pre-damaged OrF length should be used (Massaro-Giordano et al., 1998; Joseph and Glavas, 2011). In complete destruction of the IOR and OrF, the implant size is extremely difficult to measure. Pathological conditions with complete bony damage are high-velocity injuries (Markiewicz and Bell, 2012), such as the combined intraorbital and orbital rim fractures (Reyes et al., 2013) and gunshots (Liliav and Kalimuthu, 2012). In these cases of emergency, our formulas can calculate the length before the damage in each individual and each orbit directly and with accuracy.

In addition, our formula is applicable in different pathological entities with osteolytic lesions (benign and malignant tumors and infections) of the orbit (Lambertucci et al., 2009; Razek, 2011; González Ballester et al., 2012; Yan et al., 2012).

The current study has some limitations:

1. No study exists with the same design in order to compare our results
2. The number of dry skulls is representative, but a higher number of skulls might lead to a formula with more variables and a higher statistical power
3. The formula calculates only the linear distance of the OrF length without estimating the bony contour of the OrF
4. The study was conducted on dry skulls and its application on CT scans is unknown
5. The formulas' application requires intact medial, superior and lateral OrWs.

5. Conclusions

Orbital repair using the appropriate implant size is fundamental. The calculation of the OrF length in cases of complete destruction of the IOR and OrF is extremely challenging. The presented formulas are an easy and applicable method for the calculation of the OrF length by using gender and the lengths of the medial, superior and lateral OrWs of the same orbit. Such data may improve surgery planning of orbital floor fractures and complex orbital reconstructions.

Ethics statement

Skulls data were used. They belonged to body donators which donated their bodies after written informed consent to the Departments of Anatomy of Medical Schools in Greece.

Disclosure

All authors have participated in the research and the article preparation. KN and MP planned the project, GP and GS searched the literature, MP, GP and GS prepared the manuscript. GT and MP made the statistical analysis and data interpretation. All the authors approved the final form of the paper.

Conflicts of interest

The authors declare that they have no conflicts of interest.

Acknowledgements

The authors thank Miss Repousi Elpida for her valuable assistance with the statistical analysis of the paper.

References

Balasubramanian T: Orbital disorders. In: Selected Works (ed), Otolaryngology online, e-book, vol. 3; 2011, http://works.bepress.com/drtbalu/46; 2011

Bell RB, Markiewicz MR: Computer-assisted planning, stereolithographic modeling, and intraoperative navigation for complex orbital reconstruction: a descriptive study in a preliminary cohort. J Oral Maxillofac Surg 67: 2559–2570, 2009

Fang JJ, Liu JK, Wu TC, Lee JW, Kuo TH: Complex facial deformity reconstruction with a surgical guide incorporating a built-in occlusal stent as the positioning reference. J Craniofac Surg 24: 260–265, 2013

González Ballester D, González-García R, Moreno García C, Ruiz-Laza L, Monje Gil F: Mucormycosis of the head and neck: report of five cases with different presentations. J Craniomaxillofac Surg 40: 584–591, 2012

Hatcher DC: CT and CBCT imaging: assessment of the orbits. Oral Maxillofac Surg Clin North Am 24: 537–543, 2012

Joseph JM, Glavas IP: Orbital fractures: a review. Clin Ophthalmol 5: 95–100, 2011

Lambertucci JR, Fonseca P, Linares DB: Invasive aspergillosis of the orbit and cavernoussinus in a patient with Aids. Rev Soc Bras Med Trop 42: 734–735, 2009
Liliav B, Kalimuthu R: Mantle design: a composite construct for orbitalfloor reconstruction. J Craniofac Surg 23: 1125–1126, 2012
Lim TC, Rasheed ZM, Sundar G: A safe and accurate method of assessing the size of implants required in orbitalfloor reconstruction. Craniomaxillofac Trauma Reconstr 5: 111–114, 2012
Markiewicz MR, Bell RB: Traditional and contemporary surgical approaches to the orbit. Oral Maxillofac Surg Clin North Am 24: 573–607, 2012
Massaro-Giordano M, Kirschner RA, Wulc AE: Orbital floor implant migration across the ethmoidal sinuses and nasal septum. Am J Ophthalmol 126: 848–850, 1998
Metzger MC, Schön R, Weyer N, Rafii A, Gellrich NC, Schmelzeisen R, Strong BE: Anatomical 3-dimensional pre-bent titanium implant for orbital floor fractures. Ophthalmology 113: 1863–1868, 2006
Nilsson J, Nysjö J, Carlsson AP, Thor A: Comparison analysis of orbital shape and volume in unilateral fractured orbits. J Craniomaxillofac Surg 46: 381–387. https://doi.org/10.1016/j.jcms.2017.12.012, 2018
Novelli G, Tonellini G, Mazzoleni F, Bozzetti A, Sozzi D: Virtual surgery simulation in orbital wall reconstruction: integration of surgical navigation and stereolithographic models. J Craniomaxillofac Surg 42: 2025–2034, 2014
Peng MY, Merbs SL, Grant MP, Mahoney NR: Orbital fracture repair outcomes with preformed titanium mesh implants and comparison to porous polyethylene coated titanium sheets. J Craniomaxillofac Surg 45: 271–274, 2017
Piombino P, Iaconetta G, Ciccarelli R, Romeo A, Spinzia A, Califano L: Repair of orbital floor fractures: our experience and new technical findings. Craniomaxillofac Trauma Reconstr 3: 217–222, 2010
Razek AA: Imaging appearance of bone tumors of the maxillofacial region. World J Radiol 3: 125–134, 2011
Reyes JM, Vargas MFG, Rosenvasse J, Arocena MA, Medina AJ, Funes J: Classification and epidemiology of orbital fractures diagnosed by computed tomography. Rev Argent Radiol 77: 139–146, 2013
Roth FS, Koshy JC, Goldberg JS, Soparkar CN: Pearls of orbitaltraumamanagement. Semin Plast Surg 24: 398–410, 2010
Szymor P, Kozakiewicz M, Olszewski R: Accuracy of open-source software segmentation and paper-based printed three-dimensional models. J Craniomaxillofac Surg 44: 202–209, 2016
Turvey TA, Golden BA: Orbital anatomy for the surgeon. Oral Maxillofac Surg Clin North Am 24: 525–536, 2012
Yan J, Zhou S, Li Y: Benign orbital tumors with bone destruction in children. PLoS One 7: 32111, 2012